Chemistry–A European Journal
Research Article
doi.org/10.1002/chem.202103609
Chemistry Europe
European Chemical Societies Publishing
www.chemeurj.org

Merging of a Perylene Moiety Enables a Ru^{II} Photosensitizer with Long-Lived Excited States and the Efficient Production of Singlet Oxygen

Marie-Ann Schmid[+],[a] Jannik Brückmann[+],[b] Julian Bösking,[b] Djawed Nauroozi,[b] Michael Karnahl,[a] Sven Rau,*[b] and Stefanie Tschierlei*[a]

Abstract: Multichromophoric systems based on a Ru^{II} polypyridine moiety containing an additional organic chromophore are of increasing interest with respect to different light-driven applications. Here, we present the synthesis and detailed characterization of a novel Ru^{II} photosensitizer, namely [(tbbpy)$_2$Ru((2-(perylen-3-yl)-1*H*-imidazo[4,5-*f*][1,10]-phenanthrolline))](PF$_6$)$_2$ **RuipPer**, that includes a merged perylene dye in the back of the **ip** ligand. This complex features two emissive excited states as well as a long-lived (8 μs) dark state in acetonitrile solution. Compared to prototype $[(bpy)_3Ru]^{2+}$-like complexes, a strongly altered absorption ($\varepsilon = 50.3 \times 10^3\ M^{-1}\,cm^{-1}$ at 467 nm) and emission behavior caused by the introduction of the perylene unit is found. A combination of spectro-electrochemistry and time-resolved spectroscopy was used to elucidate the nature of the excited states. Finally, this photosensitizer was successfully used for the efficient formation of reactive singlet oxygen.

Introduction

Almost unlimited energy (ca. 3×10^{24} J per year) is provided by the sun, exceeding the world's increasing energy demand by more than 10000 times.[1,2] Accordingly, there is great potential in converting sunlight into electricity or energy-rich compounds, the so-called solar fuels.[3–5]

In this context, the efficient absorption and storage of photonic energy by a suited photosensitizer is crucial. In fact, especially the photosensitizer plays a key role in every photocatalytic system[6–9] and in diverse applications like organic light-emitting diodes (OLEDs),[10,11] dye-sensitized solar cells (DSSCs)[12,13] or in photodynamic therapy (PDT).[14,15] For these applications, transition metal complexes based on polypyridine ligands are still frequently used.[5,7,16–19] However, their lack of high extinction coefficients in a broad range of the visible region is a major drawback,[19–21] which needs to be tackled. One possible solution is the design of multichromophoric architectures containing organic dyes like naphthalene,[22,23] 4*H*-imidazole,[24–26] naphtalimide,[27–31] pyrene[32–36] or oligothiophene (Figure 1).[37,38] All of them already successfully demonstrated their ability to increase excited-state lifetimes and to broaden the absorption profile of the corresponding transition metal complexes. Moreover, the concept of merging an additional organic chromophore (Figure 1) with a metalorganic chromophore also resulted in complexes with high emission quantum yields and an increased electron storage capability.[21,27,28,39] In addition, these organic dyes can serve as an energy reservoir due to excited-state energy transfer processes[40–42] and are

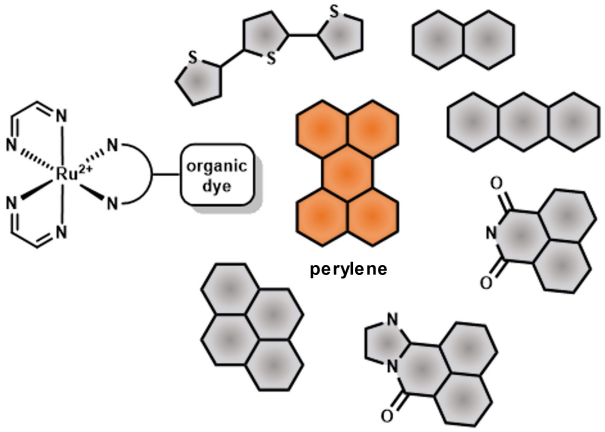

Figure 1. General concept of creating multichromophoric Ru^{II} photosensitizers by the incorporation of an additional organic dye like oligothiophene, naphthalene, anthracene, naphthalimides, pyrene (all grey, arranged clockwise) or perylene (orange, this study) into the diimine ligand.

[a] *M.-A. Schmid,[+] Dr. M. Karnahl, Prof. Dr. S. Tschierlei*
Department of Energy Conversion
Institute of Physical and Theoretical Chemistry
Technische Universität Braunschweig
Rebenring 31, 38106 Braunschweig (Germany)
E-mail: s.tschierlei@tu-bs.de

[b] *J. Brückmann,[+] J. Bösking, Dr. D. Nauroozi, Prof. Dr. S. Rau*
Institute of Inorganic Chemistry, Ulm University
Albert-Einstein-Allee 11, 89081 Ulm (Germany)
E-mail: sven.rau@uni-ulm.de

[+] *These authors contributed equally to this work.*

Supporting information for this article is available on the WWW under https://doi.org/10.1002/chem.202103609

highly active for the evolution of singlet oxygen needed for PDT applications.[14,15,43] In particular, rylene dyes like naphthalene or perylene (monoimide or diimide) are one of the most important classes of organic dyes, because they offer a broad synthetic variability, high chemical and photochemical stability as well as flexible photophysical and electrochemical properties.[44–46] In particular, rylene imide architectures were successfully incorporated to facilitate charge transfer transitions to or from the organic chromophore system.[47–52]

Rylene radical anions or cations can be observed with characteristic absorption bands. Hence, embedding of such rylene based dyes (organic chromophores) into traditional polypyridine ligands for the preparation of improved transition metal complexes is of high interest.[21,53–55]

Therefore, the new **ipPer** (2-(perylen-3-yl)-1*H*-imidazo[4,5-*f*][1,10]phenanthroline) ligand containing a perylene moiety in the backbone of the 1*H*-imidazo[4,5-*f*][1,10]phenanthroline (**ip**) and its corresponding Ru^{II} complex $[(tbbpy)_2Ru(ipPer)](PF_6)_2$ (**RuipPer**; Scheme 1) were developed within this study. A combination of electrochemical and photophysical measurements including time-resolved emission as well as nanosecond transient absorption spectroscopy was then used to evaluate the effect of the additional perylene moiety on the electrochemical and photophysical properties.

Results and Discussion

Synthesis and structural characterization

The preparation of the novel imidazophenanthroline perylene (**ipPer**) ligand was achieved by the conversion of the formylated perylene with 1,10-phenanthroline-5,6-dione (Scheme 1). Adapted Radziszewski conditions[56] for the preparation of imidazole derivatives were applied (see Chapter 2 in the Supporting Information) to minimize the formation of by-products. However, tedious washing with diethyl ether and recrystallization in chloroform was essential for purification resulting in a final yield of 66% for **ipPer**. Following, standard reaction conditions were applied for the complexation of the hardly soluble **ipPer** ligand with the $[(tbbpy)_2Ru(Cl)_2]$ precursor (tbbpy = 4,4′-tert-butyl-2,2′-bipyridine) to obtain **RuipPer**. The coordination reaction was performed under microwave irradiation either in hot ethylene glycol or in a mixture of ethanol/water (3:1, *v*:*v*) with addition of potassium hydroxide.[57,58] Purification was performed by Sephadex™ size-exclusion column chromatography with methanol. With both solvent mixtures yields of up to 80% could be achieved.

Subsequently, **ipPer** and **RuipPer** were fully characterized by ^1H and ^{13}C NMR spectroscopy and high-resolution mass spectrometry (HRMS, MALDI; see all spectra in the Supporting Information). In the ^1H NMR spectra almost all perylene protons of **ipPer** show a different chemical environment (Figure S3.1 in the Supporting Information).[28] Further, the ^1H NMR spectra of **RuipPer** exhibit solely a weak concentration dependency (in the range of 0.25 to 38.9 mM), which argues against strong π–π interactions of neighboring perylene moieties (Figure S3.8). Indeed, the perylene and also the imidazophenanthroline protons do not provide sufficient NMR shifts for the calculation of association constants.[59] 2D NMR spectroscopy (Figure S3.6) identifies the most downfield shifted aromatic proton at about 9.2 ppm as a perylene proton.

Electrochemical properties

The redox properties of **RuipPer** and of a suitable reference complex, namely $[(tbbpy)_2Ru(ip)]^{2+}$ (**Ruip**) without an additional perylene sphere at the ip moiety, were studied by cyclic and differential pulse voltammetry (CV and DPV) in corresponding acetonitrile (Figure 2 and Table 1) and *N*,*N*-dimethylformamide (DMF) solutions (Figure S5.1–2). **Ruip** was structurally characterized before,[60] but a detailed electrochemical analysis was not performed so far.

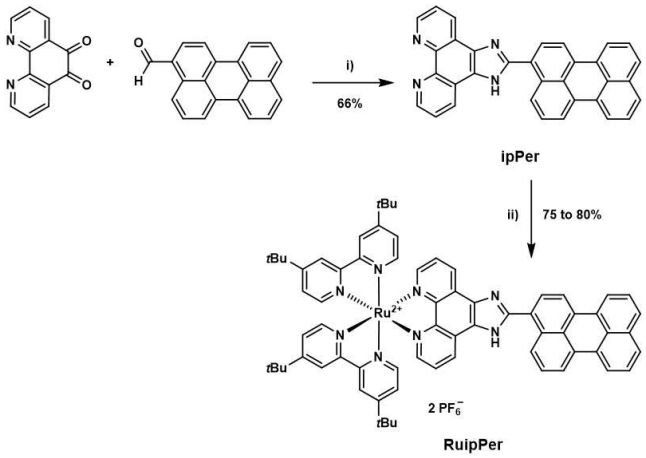

Scheme 1. Preparation of the **ipPer** ligand and its corresponding Ru^{II} complex **RuipPer**. Conditions: i) AcOH, NH_4OAc, 100 °C, 1 h, 66%; ii) $[(tbbpy)_2Ru(Cl)_2]$, ethylene glycol, 160 °C, 1.5 h, 75% or ethanol/water (3:1, *v*/*v*), $KOH_{(aq)}$, 100 °C, 2 h, 80%.

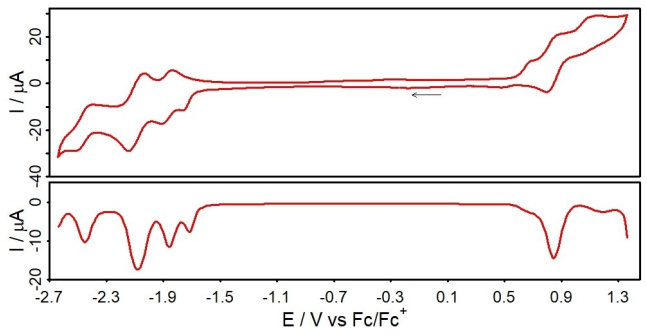

Figure 2. Cyclic voltammogram (top) and differential pulse voltammogram (bottom) of **RuipPer** (red; 1 mM) in acetonitrile solution referenced vs. the ferrocene/ferricenium (Fc/Fc^+) couple. An additional voltammogram until −3.0 V is shown in Figure S4.3. Conditions: scan rate of 100 mV/s, $[(nBu)_4N]PF_6$ (0.1 M) as supporting electrolyte. The arrow illustrates the initial scan direction.

Table 1. Summary of the electrochemical properties of **ipPer**, **RuipPer** and some reference compounds in acetonitrile solution at room temperature. Owing to solubility issues, the electrochemical characterization was also performed in deaerated DMF solutions containing 0.1 M $[(n\mathrm{Bu})_4\mathrm{N}]\mathrm{PF}_6$ as supporting electrolyte. The redox potentials are referenced versus the ferrocene/ferricenium (Fc/Fc^+) couple. E_{ox} and E_{red} = potentials of the redox processes.

Compound	E_{ox} [V]	E_{red} [V]
ipPer[a]	0.59; 0.91	−1.98; −2.15; −2.48; −2.84
RuipPer[a]	0.65; 0.81	−1.84; −1.88; −2.07;[b] −2.32; −2.53;[b] −2.82
RuipPer	0.55; 0.82;[b] 1.10	−1.76; −1.88;[b] −2.10;[b] −2.47;[b] −2.70;[d] −2.93[d]
$[(\mathrm{tbbpy})_3\mathrm{Ru}]^{2+}$[c]	0.73	−1.80; −2.01; −2.28
Ruip	0.52; 0.79[b]	−1.85;[b] −2.01; −2.09;[b] −2.43[b]

[a] Measured in DMF. [b] Reversible processes with half-wave potentials ($E_{1/2red}$), [c] Taken from ref. [61]. [d] See Figure S4.3.

The reversible oxidation of **RuipPer** from a Ru^{II} to a Ru^{III} state occurs at 0.82 V and is thus anodically shifted by 30 or 90 mV compared to **Ruip** and $[(\mathrm{tbbpy})_3\mathrm{Ru}]^{2+}$, respectively (Table 1).[61] However, in **RuipPer** this oxidation process is merged with an irreversible oxidation event of the perylene moiety at 0.55 V which corresponds well with bare perylene.[62] At 1.1 V, a second irreversible oxidation of the perylene unit occurs. Interestingly, **Ruip** exhibits an irreversible oxidation at 0.52 V consistent with the literature,[63] which is most likely related to an oxidation of the imidazole unit without substitution at its C2 carbon atom.

The cyclic voltammogram of **RuipPer** exhibits six reduction events between −1.76 V and −2.93 V (Figures 2 and S4.3.). From those, the events at −1.88, −2.10, and −2.47 V correspond well with **Ruip** and $[(\mathrm{tbbpy})_3\mathrm{Ru}]^{2+}$ and can be assigned to the progressive reduction of the phenanthroline and the two bipyridine ligand spheres, respectively.[64] Furthermore, the imidazole unit is quasireversibly reduced at −1.76 V for **RuipPer**, whereas it is cathodically shifted by 250 mV for **Ruip**. This implies that the covalently connected perylene unit would lead in a more reducible imidazole unit, which is unexpected because higher electron density on the perylene moiety should cause the opposite. This could indicate an electronically decoupled ground state.

By introduction of the perylene moiety in RuipPer, the reduction at −2.10 V assigned to the tbbpy ligand is overlapping with the first irreversible perylene reduction. (see DPV in Figure 2). At higher cathodic potentials, the perylene sphere is again reduced irreversibly (Table 1).

Photophysical properties

The photophysical properties of **ipPer** and its corresponding Ru^{II} complex **RuipPer** were studied in acetonitrile solution (Figure 3). The **ipPer** ligand exhibits an absorption maximum at around 457 nm without a characteristic vibronic fine structure, which is otherwise typical of a perylene chromophore.[62]

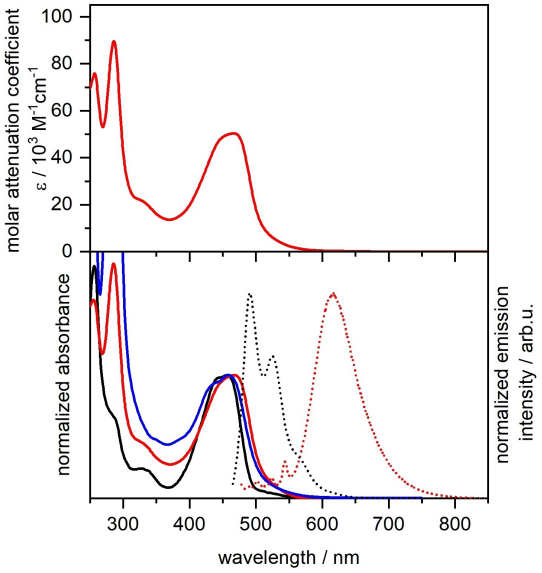

Figure 3. Top: Molar attenuation coefficients of **RuipPer** in acetonitrile solution. Bottom: Normalized absorbance (solid line) and emission (dotted) spectra of **ipPer** (black), **RuipPer** (red), and **Ruip** (blue) in acetonitrile excited at λ_{ex} = 455 nm (**ipPer**) and 468 nm (**RuipPer**).

Furthermore, its absorption profile is red-shifted of about 15 nm compared to bare perylene.[62]

With a molar extinction coefficient of $\varepsilon = 50.3 \cdot 10^3\ \mathrm{M^{-1}\ cm^{-1}}$ at 467 nm the absorptivity of **RuipPer** corresponds well to the sum of perylene π–π* ($37.0 \cdot 10^3\ \mathrm{M^{-1}cm^{-1}}$)[62] and Ru^{II} metal-to-ligand charge transfer (MLCT) transitions (17.5 $10^3\ \mathrm{M^{-1}cm^{-1}}$)[60] indicating the multichromophoric behavior of this novel complex. The intense absorption between 400 and 500 nm is again slightly red-shifted by 10 nm compared to both bare perylene and $[(\mathrm{tbbpy})_2\mathrm{Ru(ip)}]^{2+}$. In contrast to the highly emissive **ipPer** ligand (λ_{em} = 491 and 525 nm, Figure 3) the **RuipPer** complex does not show significant emission in the presence of oxygen (see Figure S5.2). Under inert conditions, however, the complex exhibits a clear emission with a maximum at 605 nm (Figure 3). Thus, the emission of **RuipPer** is oxygen sensitive (see below).

Subsequently, the effect of protonation and deprotonation of the imidazole unit of **ipPer** on the absorption and emission behavior of both the ligand itself and **RuipPer** was tested. In this context, the addition of trifluoroacetic acid (TFA) or tetrabutylammonium hydroxide (TBAOH) to acetonitrile solutions under argon atmosphere of **ipPer** and **RuipPer** was performed (Figure S5.3). For the present compounds, acidification (protonation) induces only small changes in the absorption (Figure S5.3), but a decrease in intensity and a red-shift (for **RuipPer** of about 20 nm) of the emission maxima. In contrast, for prototype complexes bearing no additional chromophore studied in aqueous solution, pH values below the pK_a value of the **ip** proton led to an increase in emission

intensity.[69] Earlier results of Ru^{II} complexes bearing an **ip** framework with a pyrene moiety revealed increased ligand centered (LC) absorptions due to protonation.[70]

Even more drastic are the effects for the deprotonation of **ipPer** and **RuipPer**. In this case, the absorption maximum of **ipPer** is shifted from 457 (neutral) to 479 nm (deprotonated, Figure S5.5). Instead, for **RuipPer** the addition of TBAOH only slightly affects the merged LC/MLCT transitions at around 460 nm, but an additional absorption band in the range from 550 to 750 nm appears (Figure S5.3). This exceeds by far the previous observed effects for pyrene substituted complexes, where usually red-shifted transitions with mostly MLCT character at about 457 nm were detected.[70]

Deprotonated **ipPer** and **RuipPer** also possess significant differences in their emission behavior. For the neutral **ipPer** the vibronically shaped emission between 470 and 580 nm is shifted to 617 nm with a broad emission profile upon deprotonation. In contrast, the emission of **RuipPer** is completely quenched upon addition of base (Figure S5.3), which is in line with literature.[69–71] Together with the emission changes upon protonation, this suggested possible quenching abilities of the differently charged imidazole moiety upon addition of acid or base.[69]

The pH dependent changes of **RuipPer** are reversible in acetonitrile solution in the presence of oxygen (Figure S5.4). When the complex is protonated by TFA (pH ≈ 3) the emission is enhanced, as in the prototype complex (Figure S5.4).[69] At the same time the absorption is not altered. Subsequently, when the complex is deprotonated again by TBAOH (pH ≈ 11), the emission is quenched and the absorption is significantly changed, shifting the MLCT absorption band to higher energies (450 nm). Upon the re-addition of TFA the absorption is red-shifted again and the stronger emission is regained. The same behavior as described above is observed, when the pH is shifted back to 11.

Time-resolved spectroscopy

The emission lifetime of **RuipPer** was detected as a biexponential decay with two time constants of 380 ns and 1500 ns in acetonitrile solution under inert conditions. The amplitudes of the global analysis illustrate that the second lifetime is more prominent (Figure 4). The first lifetime of **RuipPer** is in the same time period as ^{3}MLCT-based lifetimes for structurally related complexes, like **Ruip** (Table 2, Figure S6.1).[38,72,73] Complexes with an attached pyrene moiety typically exhibit a rather long second lifetime (e.g., 1.5 to 26 µs).[32,33,72,74] Hence, the second lifetime of **RuipPer** is with about 1.5 µs in good agreement with the literature.

This long lifetime was assigned by Reichardt and co-workers to a triplet energy equilibrium between the ^{3}MLCT and the ^{3}IL (intra-ligand) state located on the pyrene moiety.[32,33,72] This delayed emission of the ^{3}MLCT is common for multichromophoric transition metal complexes.[40] The shape of the amplitude of the second emission lifetime supports the idea, that this time constant is also related to an emission from the ^{3}MLCT state (Figure 4).

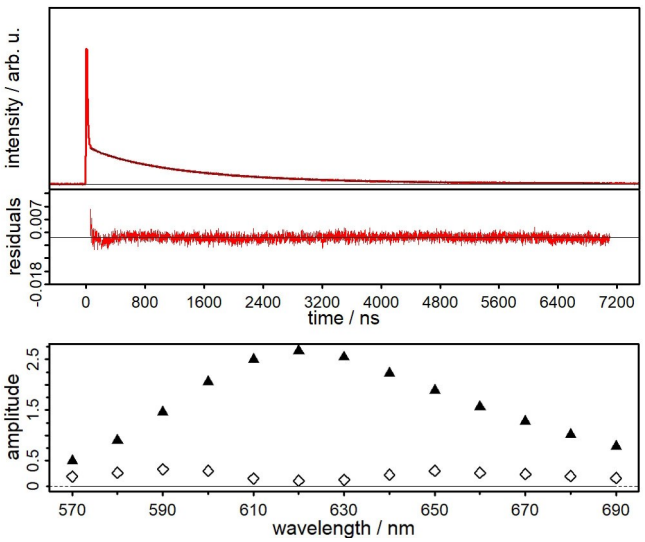

Figure 4. Emission lifetime kinetics of **RuipPer** in acetonitrile solution under inert conditions excited at 355 nm and recorded at the emission maximum. The lifetimes were determined from a biexponential fit (black) resulting in the time constants $\tau_1 = 362$ ns and $\tau_2 = 1516$ ns (top). The amplitudes are plotted in squares (a1) and triangles (a2; bottom). Global analysis yields the times $\tau_1 = 380$ ns and $\tau_2 = 1500$ ns.

Table 2. Summary of the photophysical properties of **ipPer**, **RuipPer** and some reference compounds in acetonitrile solution at room temperature. All emission properties and the quantum yield were determined under inert conditions.

Compound	$\lambda_{max,abs}$ [nm] (ε [10^3 $M^{-1}cm^{-1}$])	$\lambda_{max,em}$ [nm]	τ_{em} [ns]	τ_{tA} [ns]	Φ_{em}
ipPer	257; 288; 328; 442; 457	491; 525			
RuipPer	257 (75.8); 286 (89.6); 467 (50.3)	617	380; 1500	600; 1500; 8000	0.010
$[(bpy)_3Ru]^{2+}$[65–68]	451 (13.0)	607	1100		0.095
Ruip[60]	459 (17.5)	615	540[a]	–	–

[a] Data for **Ruip** were taken from ref. [60], except for τ_{em} (measured by us).

Interestingly, transient absorption (tA) spectroscopy revealed three lifetimes of 600 ns and 1500 ns as well as a long lifetime of 8 µs for **RuipPer** in acetonitrile solution under inert conditions (Figure 5), which is similar to other multichromophoric Ru^{II} complexes.[32,38,72]

The transient absorption spectrum of **RuipPer** has two excited state absorptions (ESA between 360 and 380 nm as well as at 450 nm; Figure 5). In addition, two ground state bleaches (GSB) until 440 and 500 nm can be seen. In this region the GSB and the ESA are superimposed. Additionally, a broad ESA from 500 to 765 nm occurs. This ESA is strong up to 660 nm with a maximum at around 570 nm. Between 660 and 760 nm the ESA appears to be rather flat (Figure 5). Interestingly, this fine structure of the tA is not changed preparing the sample under

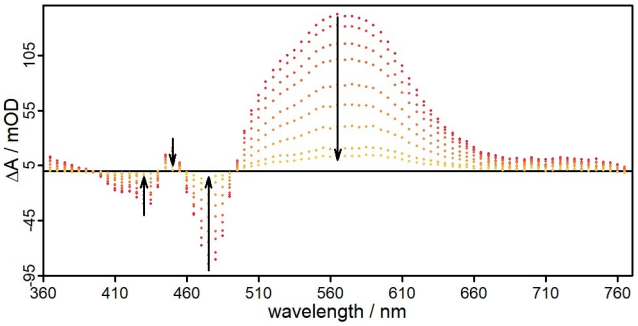

Figure 5. Nanosecond transient absorption spectra of **RuipPer** at 500, 1000, 2000, 3000, 5000, 7000, 10000, 15000, and to 18000 ns (from red to yellow) upon pumping at 355 nm (in acetonitrile, $OD_{355\,nm} = 0.3$).

oxygen, while the lifetime is drastically diminished to 150 ns (Figure S7.2). This tA spectrum is more fine structured then the tA spectrum of the Ru^{II} imidazophenanthroline pyrene complex,[72] which has a GSB before 410 nm and a broad, unstructured ESA up to 710 nm.

The uncoordinated **ipPer** ligand only exhibits strong fluorescence with a lifetime shorter than 8 ns, which is below the detection limit of our instruments.

After the general discussion of the time-resolved dynamics of **RuipPer**, we will now elaborate on the fact that it shows two emissive and one dark lifetime. In contrast to other multi-chromophoric examples,[27,33,41,72] the perylene chromophore in **RuipPer** should provide a triplet state too low in energy (1.53–1.56 eV)[75,76] to interact with the high-energy ^{3}MLCT excited states of the Ru^{II} polypyridine moiety (2.05 eV) by triplet-triplet energy transfer processes.[40,41] Thus, several possibilities of both the second emissive triplet state as well as the dark lifetime exist. First, higher-lying perylene triplet states might interact with the ^{3}MLCT (2.05 eV) states.[77] Second, the heavy metal ruthenium might induce a higher spin orbit coupling to facilitate perylene-based intersystem crossing from ^{1}LC to ^{3}LC, as observed for particular rylene-metal assemblies.[77,78] Third, charge separation and recombination processes leading to a ligand-centered triplet state may be taken into consideration.[48] Therefore, we applied spectro-electrochemical measurements to determine the photophysical properties of the reduced and oxidized species. Furthermore, we calculated the electrochemical potentials of the excited states of the respective chromophores. Finally, we explored the triplet state energy transfer capability of **RuipPer**.

Elucidation of the nature of the excited states

First, UV/vis spectro-electrochemistry was performed in acetonitrile solution containing 0.1 M $[(n\mathrm{Bu})_4\mathrm{N}]PF_6$ as supporting electrolyte. For an easier assignment and distinction of the occurring absorption bands of **RuipPer** the reference complex **Ruip** was also examined.

When **RuipPer** is oxidized at 0.8 V, a superposition of a decrease in absorption at 450 nm and a sharp peak at 530 nm becomes visible (Figure S9.1). This can be assigned to the oxidation of the ruthenium center[79] and the formation of a perylene cation, respectively.[76] At an even higher oxidation potential of 1.0 V the depletion of the MLCT absorption band due to the oxidation of Ru^{II} to Ru^{III} is more pronounced, while the formation of the perylene cation is still present (Figure S9.1). This observation is in line with the reference complex **Ruip** without a perylene moiety, where oxidation only causes a depletion of the absorption at 450 nm (Figure S9.3).

Under reductive conditions (below −1.7 V vs. Fc/Fc^+) an absorption at 530 nm is rising for both **Ruip** and **RuipPer**. Hence, this can be attributed to the reduction of the tbbpy ligands and the ip moiety (Figure S9.2 and S9.4). In the differential optical density spectrum of **RuipPer** applying higher reduction potentials below −2.0 V, a sharp absorption band at 620 nm is rising. Consequently, this feature can be assigned to a perylene anion (Figure S9.2), although the wavelength is slightly shifted compared to previous reports.[80,81]

For the estimation of the driving force for the formation of either a radical anion or cation on the perylene moiety of **RuipPer**, the electrochemical potentials of the excited states were calculated using the simplified Rehm-Weller equation (Supporting Information chapter 9).[82] Therefore, it was assumed that the two chromophoric units do not interact as it can be seen by the superposition of both the ground state photophysics and the electrochemical properties. Subsequently, the excited state electrochemical potentials were estimated from the ground state electrochemical potentials and the spectroscopic energy $E^{\circ\circ}$ related to the involved transition.[16,82] The electron donor ability of the Ru^{II} moiety in the excited state was determined with $E_{ox}^* = -1.23$ eV (0.82–2.05 eV = −1.23 eV). This driving force is too small to initiate an electron transfer towards the hardly reducible perylene moiety. The perylene can only be reduced from potentials of −2.10 V or more negative against Fc/Fc^+ (Table 1).

As a second option the perylene might act as an electron donor moiety in its excited state. Taking the relative absorptions of the two chromophores, that is, of perylene and of the Ru^{II} polypyridine center into consideration, excitation at 355 nm (as conducted in the transient absorption experiments) possibly produces excited states of both the perylene and the Ru^{II} chromophore (Figure 5). The electron donor capability of the excited perylene moiety is estimated to be −2.27 eV (= 0.55–2.82 eV). Thus, the excited state of perylene can possibly reduce the ground state Ru^{II} polypyridine states (lowest reductive redox potential of −1.76 V) to produce a charge separated state of $Ru^{II}(tbbpy)^{\bullet-}$ (**ipPer**)$^{\bullet+}$.

Upon comparison of the spectro-electrochemical features of the perylene radical cation (Figure S9.1) with the signatures observed in the transient absorption (Figure 5) we conclude that no charge separated state is visible in the nanosecond time regime. This is consistent with intramolecular Ru^{II}-rylene-based radical cationic species which recombine within the sub-100 ps timescale. Thus, from the above-mentioned options of excited state dynamics, the triplet state formation is left. The perylene based triplet state typically absorbs at around 500 nm.[83] However, in our case, this triplet state is not fully visible due to

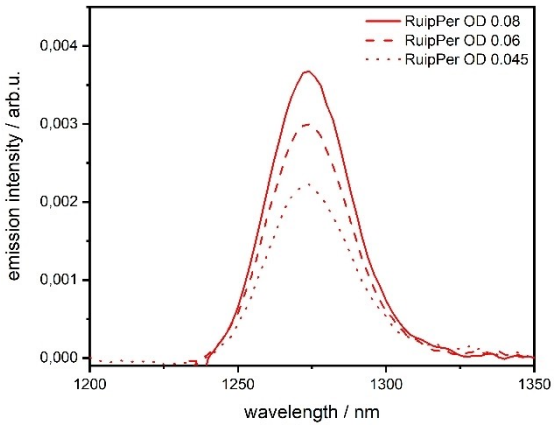

Figure 6. Direct detection of the $^1O_2$ production upon irradiation of **RuipPer** in acetonitrile solution (at different optical densities, $\lambda_{ex} = 450$ nm) by measuring its characteristic NIR emission.

the superposition of the GSB and the ESA. The small ESA at 450 nm is the beginning of a shoulder, which is not visible due to the strong GSB from 460 to 490 nm.

Based on these findings we propose that the long dark lifetime stems from a triplet state on the perylene moiety. This assumption is further supported by the fact, that the fine structure is not altered throughout the tA experiments upon addition of oxygen.

Singlet oxygen evolution

The above-mentioned oxygen-dependent emission properties of **RuipPer** indicate the participation of triplet excited states. Such effects can be used, for example, for the formation of reactive oxygen species (ROS) like singlet oxygen ($^1O_2$), which are important for PDT applications.[15,84,85] In type II reactions of PDT-related photosensitizers, energy transfer reactions from the excited, light-absorbing unit to dioxygen produces highly reactive $^1O_2$.[15] In recent years, the extraordinary reactivity of such energy transfer reactions of organic triplet states achieved by the participation of transition metal complexes has attracted increasing interest.[14,21,35,86] The most prominent example, TLD1433, is a Ru^{II} polypyridine complex bearing a terthiophene backbone that has entered clinical trials for PDT applications. As the highly reactive organic triplet states of such multichromophoric complexes like TLD1433[38,56] and Ru^{II} pyrene[35,87] induce the efficient production of $^1O_2$, **RuipPer** was also investigated for this ability by using NIR emission spectroscopy (Figure 6). The characteristic emission of $^1O_2$ at 1274 nm was referenced to $[Ru(bpy)_3]^{2+}$ ($\Phi(^1O_2) = 57 \pm 5\%$) and resulted in a singlet oxygen quantum yield of $80 \pm 6\%$ for **RuipPer**. This excellent value is well comparable with leading compounds such as TLD1433 (77%) or the corresponding quaterthiophene-substituted Ru^{II} complex with a $^1O_2$ quantum yield of 81%.[38]

Conclusion

In this study, a novel multichromophoric photosensitizer based on a Ru^{II} polypyridine unit that is merged with an additional perylene moiety was successfully developed. Photophysical measurements revealed a strong absorptivity with high molar extinction coefficients (e.g., $\varepsilon = 50.3 \times 10^3\ M^{-1}\,cm^{-1}$ at 467 nm) derived from a superposition of the absorption properties of both chromophores. Moreover, the absorption and emission properties of **RuipPer** are strongly affected by the protonation state of the ip moiety; the deprotonation has an especially drastic impact. Upon excitation with visible light, **RuipPer** exhibits altered excited-state properties and increased singlet oxygen quantum yields of $80 \pm 6\%$ compared to prototype complexes like $[(bpy)_3Ru]^{2+}$. Furthermore, we propose that the long-lived excited states are triplet states because the characteristic spectral features of the perylene radical anion or cation in the spectro-electrochemical measurements do not match the states observed in the tA spectra. Either charge separation and recombination processes lead to an excited triplet state on the perylene moiety or the direct interaction of the sensitized ^{3}MLCT excited states with energetically higher lying perylene triplet states are responsible for the increased excited-state lifetime of 8 μs. The existence of a triplet excited state is further corroborated by the preserved fine structure obtained in the transient absorption measurements in the presence of oxygen as well as by the quenching of the lifetime. In total, **RuipPer** offers two emissive ^{3}MLCT states, an initial ^{3}MLCT of 380 ns and a second delayed ^{3}MLCT of 1500 ns interacting with the ^{3}IL. A third dark perylene-based excited state has a lifetime of 8 μs.

Detailed future investigations using various techniques should continue with the study of the short-lived species finally ending in the long-lived excited states explored herein. Ultrafast spectroscopic techniques and the detection of the possible radical charge separated species by, for example, EPR spectroscopy along with theoretical simulations of the excited states would clarify the ongoing processes.

Experimental Section

Further synthetic details, ^{1}H and ^{13}C NMR spectra, mass spectrometric data and cyclic voltammograms are provided in the Supporting Information. Also, additional results of steady-state absorption, emission, time-resolved emission, transient absorption spectroscopy and spectro electrochemistry are presented.

Acknowledgements

J. Brückmann gratefully acknowledges the Fonds der Chemischen Industrie (FCI) for a Kekulé-Stipendium. M.-A.S. is thankful to the Baden-Württemberg Foundation (BW-Stiftung) for financial support. This work was further supported by the Deutsche Forschungsgemeinschaft (DFG) within the Priority Program SPP 2102 "Light-controlled reactivity of metal complexes" (KA 4671/2-1 and TS 330/4-1) and within the collaborative research center TRR 234 "Catalight" Projektnummer

364549901–TRR 234 [A1 and A3]. Open Access funding enabled and organized by Projekt DEAL.

Conflict of Interest

The authors declare no conflict of interest.

Data Availability Statement

The data that support the findings of this study are available in the supplementary material of this article.

Keywords: excited-state properties · perylene · ruthenium polypyridine · singlet oxygen · spectro-electrochemistry

[1] N. Armaroli, V. Balzani, *Angew. Chem. Int. Ed.* **2007**, *46*, 52–66; *Angew. Chem.* **2007**, *119*, 52–67.
[2] N. Armaroli, V. Balzani, *Chem. Eur. J.* **2016**, *22*, 32–57.
[3] S. Styring, *Faraday Discuss.* **2012**, *155*, 357–376.
[4] E. S. Andreiadis, M. Chavarot-Kerlidou, M. Fontecave, V. Artero, *Photochem. Photobiol.* **2011**, *87*, 946–964.
[5] S. Berardi, S. Drouet, L. Francàs, C. Gimbert-Surinach, M. Guttentag, C. Richmond, T. Stoll, A. Llobet, *Chem. Soc. Rev.* **2014**, *43*, 7501–7519.
[6] C. K. Prier, D. A. Rankic, D. W. C. Macmillan, *Chem. Rev.* **2013**, *113*, 5322–5363.
[7] Y.-J. Yuan, Z. Yu, D.-Q. Chen, Z.-G. Zou, *Chem. Soc. Rev.* **2017**, *46*, 603–631.
[8] K. Behm, R. D. Mcintosh, *ChemPlusChem* **2020**, *85*, 2611–2618.
[9] P. A. Forero Cortés, M. Marx, M. Trose, M. Beller, *ChemCatChem* **2021**, *1*, 298–338.
[10] R. D. Costa, E. Ortí, H. J. Bolink, F. Monti, G. Accorsi, N. Armaroli, *Angew. Chem. Int. Ed.* **2012**, *51*, 8178–8211; *Angew. Chem.* **2012**, *124*, 8300–8334.
[11] C. Bizzarri, E. Spuling, D. M. Knoll, D. Volz, S. Bräse, *Coord. Chem. Rev.* **2018**, *373*, 49–82.
[12] A. Hagfeldt, G. Boschloo, L. Sun, L. Kloo, H. Pettersson, *Chem. Rev.* **2010**, *110*, 6595–6663.
[13] C. E. Housecroft, E. C. Constable, *Chem. Soc. Rev.* **2015**, *44*, 8386–8398.
[14] S. Monro, K. L. Colón, H. Yin, J. Roque, P. Konda, S. Gujar, R. P. Thummel, L. Lilge, C. G. Cameron, S. A. McFarland, *Chem. Rev.* **2019**, *119*, 797–828.
[15] M. C. DeRosa, R. J. Crutchley, *Coord. Chem. Rev.* **2002**, *233–234*, 351–371.
[16] N. Armaroli, *Chem. Soc. Rev.* **2001**, *30*, 113–124.
[17] M. Schulz, M. Karnahl, M. Schwalbe, J. G. Vos, *Coord. Chem. Rev.* **2012**, *256*, 1682–1705.
[18] W. T. Eckenhoff, R. Eisenberg, *Dalton Trans.* **2012**, *41*, 13004–13021.
[19] P. D. Frischmann, K. Mahata, F. Würthner, *Chem. Soc. Rev.* **2013**, *42*, 1847–1870.
[20] S. Campagna, F. Puntoriero, F. Nastasi, G. Bergamini, V. Balzani, *Top. Curr. Chem.* **2007**, *280*, 117–214.
[21] F. N. Castellano, *Acc. Chem. Res.* **2015**, *48*, 828–839.
[22] G. E. Shillito, S. E. Bodman, J. I. Mapley, C. M. Fitchett, K. C. Gordon, *Inorg. Chem.* **2020**, *59*, 16967–16975.
[23] A. El-ghayoury, A. Harriman, A. Khatyr, R. Ziessel, *J. Phys. Chem. A* **2000**, *104*, 1512–1523.
[24] L. Zedler, S. Kupfer, I. R. De Moraes, M. Wächtler, R. Beckert, M. Schmitt, J. Popp, S. Rau, B. Dietzek, *Chem. Eur. J.* **2014**, *20*, 3793–3799.
[25] M. Wächtler, M. Maiuri, D. Brida, J. Popp, S. Rau, G. Cerullo, B. Dietzek, *ChemPhysChem* **2013**, *14*, 2973–2983.
[26] S. Kupfer, J. Guthmuller, M. Wächtler, S. Losse, S. Rau, B. Dietzek, J. Popp, L. González, *Phys. Chem. Chem. Phys.* **2011**, *13*, 15580–8.
[27] D. S. Tyson, C. R. Luman, X. Zhou, F. N. Castellano, *Inorg. Chem.* **2001**, *40*, 4063–4071.
[28] Y. Yang, J. Brückmann, W. Frey, S. Rau, M. Karnahl, S. Tschierlei, *Chem. Eur. J.* **2020**, *26*, 17027–17034.
[29] M. A. Haga, *Inorg. Chim. Acta* **1983**, *75*, 29–35.
[30] M. Borgström, N. Shaikh, O. Johansson, M. F. Anderlund, S. Styring, B. Åkermark, A. Magnuson, L. Hammarström, *J. Am. Chem. Soc.* **2005**, *127*, 17504–17515.
[31] K. A. Wells, J. E. Yarnell, S. Sheykhi, J. R. Palmer, D. T. Yonemoto, R. Joyce, S. Garakyaraghi, F. N. Castellano, *Dalton Trans.* **2021**, *50*, 13086–13095.
[32] W. E. Ford, M. A. J. Rodgers, *J. Phys. Chem.* **1992**, *96*, 2917–2920.
[33] N. D. McClenaghan, F. Barigelletti, B. Maubert, S. Campagna, *Chem. Commun.* **2002**, *2*, 602–603.
[34] D. S. Tyson, J. Bialecki, F. N. Castellano, *Chem. Commun.* **2000**, 2355–2356.
[35] R. Lincoln, L. Kohler, S. Monro, H. Yin, M. Stephenson, R. Zong, A. Chouai, C. Dorsey, R. Hennigar, R. P. Thummel, S. A. Mcfarland, *J. Am. Chem. Soc.* **2013**, *135*, 17161–17175.
[36] E. C. Constable, M. Neuburger, P. Rösel, G. E. Schneider, J. A. Zampese, C. E. Housecroft, F. Monti, N. Armaroli, R. D. Costa, E. Ortí, *Inorg. Chem.* **2013**, *52*, 885–897.
[37] J. A. Roque, P. C. Barrett, H. D. Cole, L. M. Lifshits, E. Bradner, G. Shi, D. Von Dohlen, S. Kim, N. Russo, G. Deep, C. G. Cameron, M. E. Alberto, S. A. McFarland, *Inorg. Chem.* **2020**, *59*, 16341–16360.
[38] A. Chettri, J. A. Roque, K. R. A. Schneider, H. D. Cole, C. G. Cameron, S. A. McFarland, B. Dietzek, *ChemPhotoChem* **2021**, *5*, 421–425.
[39] M. Schulz, N. Hagmeyer, F. Wehmeyer, G. Lowe, M. Rosenkranz, B. Seidler, A. Popov, C. Streb, J. G. Vos, B. Dietzek, *J. Am. Chem. Soc.* **2020**, *142*, 15722–15728.
[40] N. D. McClenaghan, Y. Leydet, B. B. Maubert, M. T. Indelli, S. Campagna, *Coord. Chem. Rev.* **2005**, *249*, 1336–1350.
[41] X. Y. Wang, A. Del Guerzo, R. H. Schmehl, *J. Photochem. Photobiol. C* **2004**, *5*, 55–77.
[42] F. Glaser, C. Kerzig, O. S. Wenger, *Angew. Chem. Int. Ed.* **2020**, *59*, 10266–10284; *Angew. Chem.* **2020**, *132*, 10266–10284.
[43] K. Szaciłowski, W. Macyk, A. Drzewiecka-Matuszek, M. Brindell, G. Stochel, *Chem. Rev.* **2005**, *105*, 2647–2694.
[44] T. Weil, T. Vosch, J. Hofkens, K. Peneva, K. Müllen, *Angew. Chem. Int. Ed.* **2010**, *49*, 9068–9093; *Angew. Chem.* **2010**, *122*, 9252–9278.
[45] F. Würthner, C. R. Saha-Möller, B. Fimmel, S. Ogi, P. Leowanawat, D. Schmidt, *Chem. Rev.* **2016**, *116*, 962–1052.
[46] C. Huang, S. Barlow, S. R. Marder, *J. Org. Chem.* **2011**, *76*, 2386–2407.
[47] D. Hayes, L. Kohler, L. X. Chen, K. L. Mulfort, *J. Phys. Chem. Lett.* **2018**, *9*, 2070–2076.
[48] R. K. Dubey, M. Niemi, K. Kaunisto, K. Stranius, A. Efimov, N. V. Tkachenko, H. Lemmetyinen, *Inorg. Chem.* **2013**, *52*, 9761–9773.
[49] R. J. Lindquist, B. T. Phelan, A. Reynal, E. A. Margulies, L. E. Shoer, J. R. Durrant, M. R. Wasielewski, *J. Mater. Chem. A* **2016**, *4*, 2880–2893.
[50] M. T. Vagnini, A. L. Smeigh, J. D. Blakemore, S. W. Eaton, N. D. Schley, F. D'Souza, R. H. Crabtree, G. W. Brudvig, D. T. Co, M. R. Wasielewski, *Proc. Nat. Acad. Sci.* **2012**, *109*, 15651–15656.
[51] V. L. Gunderson, E. Krieg, M. T. Vagnini, M. A. Iron, B. Rybtchinski, M. R. Wasielewski, *J. Phys. Chem. B* **2011**, *115*, 7533–7540.
[52] F. Nastasi, G. La Ganga, S. Campagna, Z. Syrgiannis, F. Rigodanza, S. Vitale, A. Licciardello, M. Prato, *Phys. Chem. Chem. Phys.* **2017**, *19*, 14055–14065.
[53] F. N. Castellano, *Dalton Trans.* **2012**, *41*, 8493–8501.
[54] K. Kodama, A. Kobayashi, T. Hirose, *Tetrahedron Lett.* **2013**, *54*, 5514–5517.
[55] A. Cravcenco, M. Hertzog, C. Ye, M. N. Iqbal, U. Mueller, L. Eriksson, K. Börjesson, *Sci. Adv.* **2019**, *5*, 1–5.
[56] Y. Arenas, S. Monro, G. Shi, A. Mandel, S. A. McFarland, L. Lilge, *Photodiagn. Photodyn. Ther.* **2013**, *10*, 615–625.
[57] M. Karnahl, S. Tschierlei, C. Kuhnt, B. Dietzek, M. Schmitt, J. Popp, M. Schwalbe, S. Krieck, H. Görls, F. W. Heinemann, S. Rau, *Dalton Trans.* **2010**, *39*, 2359–2370.
[58] S. Chakrabortty, B. K. Agrawalla, A. Stumper, N. M. Vegi, S. Fischer, C. Reichardt, M. Kögler, B. Dietzek, M. Feuring-Buske, C. Buske, S. Rau, T. Weil, *J. Am. Chem. Soc.* **2017**, *139*, 2512–2519.
[59] M. G. Pfeffer, C. Pehlken, R. Staehle, D. Sorsche, C. Streb, S. Rau, *Dalton Trans.* **2014**, *43*, 13307–13315.
[60] L. Petermann, R. Staehle, T. D. Pilz, D. Sorsche, H. Görls, S. Rau, *Eur. J. Inorg. Chem.* **2015**, *5*,750–762.
[61] A. K. Mengele, C. Müller, D. Nauroozi, S. Kupfer, B. Dietzek, S. Rau, *Inorg. Chem.* **2020**, *59*, 12097–12110.
[62] M. Hu, A. A. Sukhanov, X. Zhang, A. Elmali, J. Zhao, S. Ji, A. Karatay, V. K. Voronkova, *J. Phys. Chem. B* **2021**, *125*, 4187–4203.
[63] R. V. Khade, D. Choudhury, H. Pal, A. S. Kumbhar, *ChemPhysChem* **2018**, *19*, 2380–2388.

[64] Note: the electrochemical interpretation can be assigned in differently based on the following reference concluding that first the two bipyridines and afterwards the phenanthroline ligand in RuipPer get reduced, J. Bolger, A. Gourdon, E. Ishow, J.-P. Launay, *Inorg. Chem.* **1996**, *35*, 2937–2944.
[65] K. Peuntinger, T. D. Pilz, R. Staehle, M. Schaub, S. Kaufhold, L. Petermann, M. Wunderlin, H. Görls, F. W. Heinemann, J. Li, T. Drewello, J. G. Vos, D. M. Guldi, S. Rau, *Dalton Trans.* **2014**, *43*, 13683–13695.
[66] L. Favereau, A. Makhal, D. Provost, Y. Pellegrin, E. Blart, E. Göransson, L. Hammarström, F. Odobel, *Phys. Chem. Chem. Phys.* **2017**, *19*, 4778–4786.
[67] K. Suzuki, A. Kobayashi, S. Kaneko, K. Takehira, T. Yoshihara, H. Ishida, Y. Shiina, S. Oishi, S. Tobita, *Phys. Chem. Chem. Phys.* **2009**, *11*, 9850–9860.
[68] A. Juris, V. Balzani, P. Belser, A. von Zelewsky, *Helv. Chim. Acta* **1981**, *64*, 2175–2182.
[69] B. Jing, T. Wu, C. Tian, M. Zhang, T. Shen, *Bull. Chem. Soc. Jpn.* **2000**, *73*, 1749–1755.
[70] C. Reichardt, T. Sainuddin, M. Wa, S. Monro, S. Kupfer, J. Guthmuller, S. Gra, S. A. McFarland, B. Dietzek, *J. Phys. Chem. A* **2016**, *120*, 6379–6388.
[71] Z. S. Li, H. X. Yang, A. G. Zhang, H. Luo, K. Z. Wang, *Inorg. Chim. Acta* **2011**, *370*, 132–140.
[72] C. Reichardt, M. Pinto, M. Wächtler, M. Stephenson, S. Kupfer, T. Sainuddin, J. Guthmuller, S. A. McFarland, B. Dietzek, *J. Phys. Chem. A* **2015**, *119*, 3986–3994.
[73] R. Staehle, C. Reichardt, J. Popp, D. Sorsche, L. Petermann, K. Kastner, C. Streb, B. Dietzek, S. Rau, *Eur. J. Inorg. Chem.* **2015**, *2015*, 3932–3939.
[74] M. Hissler, A. Harriman, A. Khatyr, R. Ziessel, *Chem. Eur. J.* **1999**, *5*, 3366–3381.
[75] J. S. Seixas De Melo, H. D. Burrows, C. Serpa, L. G. Arnaut, *Angew. Chem. Int. Ed.* **2007**, *46*, 2094–2096; *Angew. Chem.* **2007**, *119*, 2140–2142.
[76] K. H. Grellmann, A. R. Watkins, *Chem. Phys. Lett.* **1971**, *9*, 439–443.
[77] R. D. Costa, F. J. Céspedes-Guirao, H. J. Bolink, F. Fernández-Lázaro, Á. Sastre-Santos, E. Ortí, J. Gierschner, *J. Phys. Chem. C* **2009**, *113*, 19292–19297.
[78] M. Schulze, A. Steffen, F. Würthner, *Angew. Chem. Int. Ed.* **2015**, *54*, 1570–1573; *Angew. Chem.* **2015**, *127*, 1590–1593.
[79] R. Lomoth, T. Häupl, O. Johansson, L. Hammarström, *Chem. Eur. J.* **2002**, *8*, 102–110.
[80] V. Markovic, D. Villamaina, I. Barabanov, L. M. Lawson Daku, E. Vauthey, *Angew. Chem. Int. Ed.* **2011**, *50*, 7596–7598; *Angew. Chem.* **2011**, *123*, 7738–77740.
[81] K. Kawai, N. Yamamoto, H. Tsubomura, *Bull. Chem. Soc. Jpn.* **1970**, *43*, 2266–2268.
[82] A. Juris, V. Balzani, F. Barigelletti, S. Campagna, P. Belser, A. Von Zelewsky, *Coord. Chem. Rev.* **1988**, *84*, 85–277.
[83] M. Imran, A. A. Sukhanov, Z. Wang, A. Karatay, J. Zhao, Z. Mahmood, A. Elmali, V. K. Voronkova, M. Hayvali, Y. H. Xing, S. Weber, *J. Phys. Chem. C* **2019**, *123*, 7010–7024.
[84] T. Wang, N. Zabarska, Y. Wu, M. Lamla, S. Fischer, K. Monczak, D. Y. W. Ng, S. Rau, T. Weil, *Chem. Commun.* **2015**, *51*, 12552–12555.
[85] N. M. Vegi, S. Chakrabortty, M. M. Zegota, S. L. Kuan, A. Stumper, V. P. S. Rawat, S. Sieste, C. Buske, S. Rau, T. Weil, M. Feuring-Buske, *Sci. Rep.* **2020**, *10*, 1–10.
[86] G. Shi, S. Monro, R. Hennigar, J. Colpitts, J. Fong, K. Kasimova, H. Yin, R. DeCoste, C. Spencer, L. Chamberlain, A. Mandel, L. Lilge, S. A. McFarland, *Coord. Chem. Rev.* **2015**, *282–283*, 127–138.
[87] M. Stephenson, C. Reichardt, M. Pinto, M. Wa, T. Sainuddin, G. Shi, H. Yin, S. Monro, E. Sampson, B. Dietzek, S. A. McFarland, *J. Phys. Chem. A* **2014**, *118*, 10507–10521.

Manuscript received: October 5, 2021
Accepted manuscript online: November 12, 2021
Version of record online: December 13, 2021